Journal of Pharmaceutical Research and Innovation (JPRI)
Volume 6, Issue 1, January 2026

e-ISSN: 2583-0023

A Multi-Modal Biosignal-Based Sleep Analysis Framework for Insomnia Detection

Emran Ali[1*], Fei He[2], Ahsan Habib[3], Maia Angelova[4], Chandan Karmakar[5]

[1, 3, 5] School of Information Technology, Deakin University, Melbourne, Victoria, Australia
[1,2]Centre for Computational Science and Mathematical Modelling, Coventry University, Coventry, UK.
[4]Sir Peter Rigby Digital Future Institute, Aston University, Birmingham, UK
Institute of Biophysics and Biomedical Engineering, Bulgarian Academy of Science, Sofia, Bulgaria
[*]Corresponding Author Email: emran.ali@research.deakin.edu.au

Abstract

Insomnia is the second most prevalent sleep disorder and the most difficult to diagnose. There are different sleep analysis approaches that can be used in insomnia detection that use various physiological signals. Hypnograms, on the other hand, have great potential in sleep disorder detection and have not often been used with other physiological signals for sleep analysis. In this study, we developed a novel framework that uses multimodal physiological signals, including EEG and hypnogram, to diagnose insomnia. Nonlinear time-domain features extracted from EEG and sleep stage transition features from hypnogram are used standalone and in combination to observe the efficacy of those settings. We use various machine learning models and feature selection methods for this investigation. The results found in this study indicate that the hypnogram features are a great addition to the time-domain features in insomnia detection. The performance improvement in various models ranges from 2%-12% after adding hypnogram features. This finding ultimately shows that a hypnogram can be a great addition in sleep analysis when the pattern of disorder is very complex.

Keywords

EEG, hypnogram, insomnia detection, ML, nonlinear feature, sleep disorder detection, sleep stage transition.

INTRODUCTION

Sleep represents one of the fundamental physiological phenomena vital to all living species. It facilitates systematic rejuvenation, recovery and cellular-level repair [1] [2]. However, at the neurological level, it is instrumental to critical functions such as memory transfer and consolidation, dreaming and nervous resetting [3] [4]. Despite its criticality, a significant proportion of the global population fails to achieve adequate and quality sleep, which ultimately compromises personal, social, occupational, and financial wellbeing [5] [6]. Macroeconomically, it is estimated that nations lose 1% of their total GDP due to the direct and indirect ramifications of sleep-related impairments [7] [8]. Approximately one-third of the global population is afflicted by some form of sleep disorder, which is categorized as severe in 52% of these cases [9]. Epidemiological data indicate a prevalence rate of 21% amongst males and 23% amongst females worldwide [10] [11]. Regarding the prevalence of specific sleep pathologies, insomnia is the second most common sleep disorder, following sleep disordered breathing (sleep apnea). Estimates suggest that around 30-35% of total sleep disorders are either acute or chronic insomnia [12] [13]. In acute insomnia, people suffer from sleeplessness or interrupted sleep, a few times a week or a month. On the other hand, in chronic insomnia, people suffer severe sleep disturbance or irregular waking between sleep multiple days a week. Despite being a more prevalent sleep disorder, sleep apnea is relatively easier and straightforward to detect or diagnose. However, insomnia remains one of the most elusive disorders to diagnose; this diagnostic complexity arises from its highly idiosyncratic patterns and the absence of clearly defined, objective biomarkers [14].

Current diagnostic methodologies range from subjective manual sleep diary analysis to objective physiological signal-based assessments [13] [15] [16]. Given that manual processes are notoriously labour-intensive and time-consuming, computational sleep analysis has emerged as a more viable and practical alternative. Amongst various sleep disorder detection or diagnosis techniques, polysomnography (PSG) remains the clinical gold standard for various sleep disorders [14] [17]. The PSG signal is a complex and composite physiological signal comprising electroencephalography (EEG), electrocardiography (ECG), electromyography (EMG), electrocardiography (EKG), electrooculography (EOG), and other bio signals. Instead of using PSG, which is primarily practical for clinical environments, individual components of PSG can also be used in sleep diagnosis [18] [19]. Whilst multi-lead EEG, ECG and other sensors can be used for sleep analysis, a more lightweight system could be preferable over those bulky configurations, especially for in-home applications [13] [19]. A hypnogram is such a bio signal that records the transition patterns of the sleep stages over night [20] [21]. Whilst it can be derived from clinical PSG, EEG, ECG or other physiological signals, certain wearable solutions are now capable of producing hypnograms [22] [23] [24]. Sleep dynamics or changes in the transition patterns of the sleep stages are increasingly recognized as containing latent

Journal of Pharmaceutical Research and Innovation (JPRI)
Volume 6, Issue 1, January 2026
e-ISSN: 2583-0023

information regarding an individual's systemic health [25] [26] [27] [28].

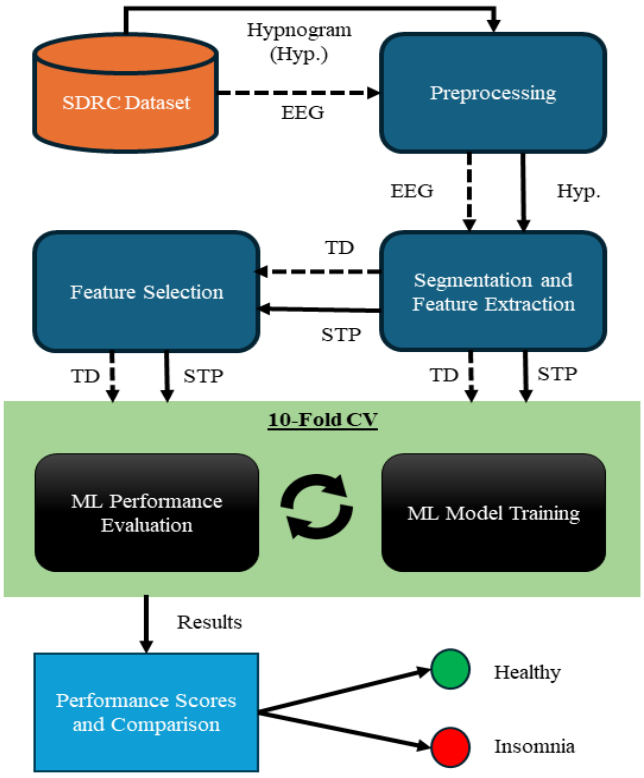

Figure 1. The block diagram of the experiment is presented in this figure, starting from data collection and preprocessing, segmentation, feature extraction, and classification

Prior research has demonstrated the utility of stage transition patterns in the analysis of various sleep disorders [27] [28] [29]. However, most of those investigations have predominantly relied upon traditional statistical methodologies to detect sleep disorders. Furthermore, the scope of existing studies has typically been restricted to either conventional physiological signals or the hypnogram in isolation; consequently, hybrid multimodal sleep analysis incorporating hypnogram dynamics remains largely unexamined. The aim of this study is to develop a robust classification model for distinguishing sleep disorders (especially, insomnia) using multimodal physiological signals, EEG and hypnogram. Additionally, this research evaluates the diagnostic sufficiency of individual modalities compared to their integrated counterparts. Finally, the study assesses the feasibility of implementing such a framework as a lightweight, in-home pre-screening system for acute insomnia, suitable for deployment beyond traditional clinical environments.

DATA AND METHODS

Data

We used one of the publicly available datasets that are commonly used for sleep stage classification and sleep disorder detection. The dataset used in this study is the Sleep-Disordered Respiratory Care (SDRC) dataset (Available on: https://data.mendeley.com/datasets/3hx58k232n/4). It has 22 subjects' recordings, with 11 subjects each from the healthy or insomniac group. Each record contains approximately 8 hours of physiological PSG signals recorded overnight. The signals include EEG, ECG, EMG, EOG, oxygen saturation (SpO2) and hypnogram. The hypnogram contains five sleep stages, namely, W (Wake), N1-N3 (Non-REM sleep stages with lighter, light and deep sleep stages) and REM (rapid-eye-movement). Each of these annotations was marked by an expert human annotator based on the Rechtschaffen and Kales (R&K) scheme/standard by observing 30-second PSG signal segments. Any human annotation error that occurred during these annotations was ignored, as there is no way to track them back since there were no indications in the dataset descriptions. The details of the datasets are shown in Table 1.

This single-night records contain various PSG components signals recorded with the channels: 'EOG1', 'EOG2', 'EOG1A1', 'EOG2A1', 'C4A1', 'C3A2', 'F3', 'F4', 'C3', 'C4', 'A1', 'A2', 'O1', 'O2', 'ECGII', 'EMG', 'EMG1', 'EMG2', 'EOG1A2', 'EOG2A2', 'F3A2', 'F4A1', 'O1A2', and 'O2A1'. However, we are only interested in observing and comparing the performance of the hypnogram signal with the EEG signal. The EEG signals from various channels were recorded with a sampling rate of 200Hz. The EEG signals were recorded from the frontal (F), central (C) and occipital (O) regions. There are two types of reference used to collect those EEG channels; 1) unipolar: 'F3', 'F4', 'C3', 'C4', 'O1', 'O2', and references ('A1', 'A2'), and bipolar: 'F3A2', 'F4A1', 'C4A1', 'C3A2', 'O1A2', and 'O2A1'.

Table 1. SDRC Dataset Description

Criteria	Description
Total subjects	22
Healthy subject	11
Sub-SD	11
Total record files	22
Average record duration	~8 hr
Available signals	EEG, ECG, EMG, EOG, SpO_2, and Hypnogram
Segment length	~30 sec
Scoring scheme	R&K
Sleep stages	W, S1, S2, S3, S4, REM

Methodology

The EEG and hypnogram signals are available in separate files in the database. After collecting the sleep data along with the EEG from the PSG file and the hypnogram from the annotation file, a basic preprocessing was performed on the raw signals. The preprocessed signals were then transferred to the data segmentation and feature extraction module. Some specific channels from each EEG signal were extracted for

Journal of Pharmaceutical Research and Innovation (JPRI)
Volume 6, Issue 1, January 2026
e-ISSN: 2583-0023

further processing. After the channel extraction from the EEG, the EEG channels' signals and the hypnogram signal were segmented with an overlapping window. Each segmented EEG channel and hypnogram were then sent to the feature extraction modules to extract the time-domain (TD) nonlinear features from the EEG and sleep stage transition probability (STP) features from the hypnogram. These features were then fed directly to the machine learning (ML) models or after selecting a few features. The results from the experiments were then analyzed and compared. We investigated how effective the TD and SPT features are in detecting insomnia, and whether they can be useful to be incorporated together in the system. A block diagram is shown in the Figure. 1 shows the methodological approach with the visual, and the next few subsections will describe the detailed processes of each block.

Preprocessing

As described earlier, there are two types of signals that we dealt with- EEG and hypnogram. Hence, separate preprocessing was done on those signals. The EEG signal extracted from the PPG signal files was preprocessed by downsampling the signals from 200Hz to 128Hz for simplicity and easy processing. After that, only the unipolar EEG channels from the central region (C3 and C4) were extracted, as the central channels were found to be more prominent for insomnia detection [15] [19]. A sample EEG signal from channel C4 is shown in the Figure. 2. On the other hand, the hypnogram annotations are converted from the legacy R&K scheme to the American Academy of Sleep Medicine (AASM) scheme as being a more commonly used approach [28]. A sample hypnogram signal presented in the AASM scheme for an insomniac subject is shown in the Figure. 3.

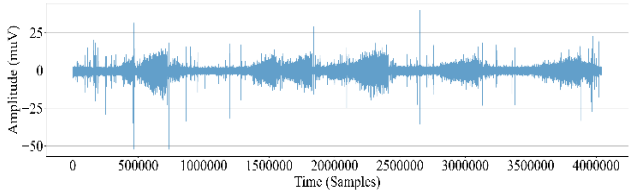

Figure 2. Sample overnight EEG signal of 8 hours (approx.) duration. It shows the C4 channel of an insomniac subject. The Y-axis indicates the amplitude of the EEG signal represented in microvolts

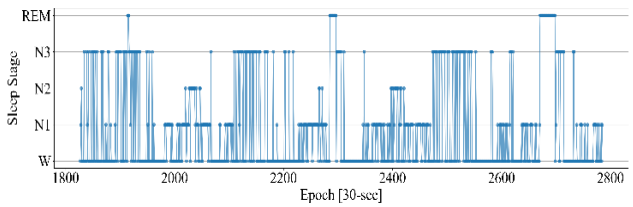

Figure 3. A sample hypnogram of an insomniac subject. The overnight hypnogram is represented in in AASM scheme

Segmentation

As described earlier, there are two types of signals that we dealt with are EEG and hypnogram. The signals from the EEG channels and hypnogram are segmented using a 90-minute-long window, and the subsequent segments were extracted by overlapping 80 minutes of the signals from the previous segment. This was we maximize the number of data points from a signal. The concept of a 90-minute window comes from the idea of a sleep cycle [30]. A healthy adult individual completes a round to go through all the sleep stages (W→N1→N2→N3→N2→REM) in 90 minutes. Hence, we expected that some kind of patterns from this sleep cycle would be captured by the ML models when this data is fed to them.

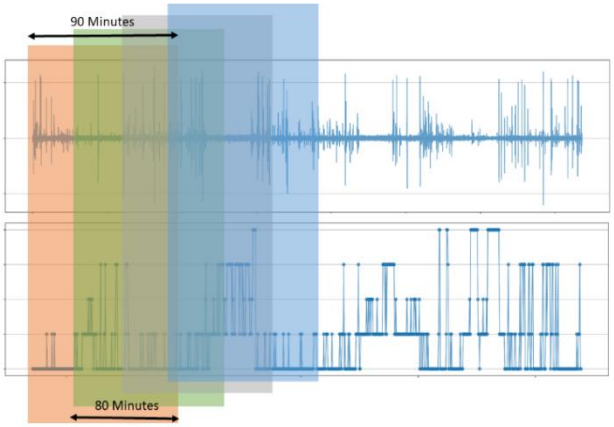

Figure 4. Segmentation of the EEG channel and the hypnogram with a 90-minute-long window with 80 minutes of overlap

Feature Extraction

Different sets of features were extracted from the segments coming from the EEG channels and hypnogram. There are plenty of features, from time, frequency, and wavelet domains, that could be extracted from the EEG signal segment. However, considering the complexity and dynamic nature of EEG, we extracted some TD nonlinear (complexity and fractal) features from time domain for analysis using a feature extractor library developed by us [31]. We used the lempelZivComp, hjorthMob, hjorthComp, fisherInfo, petrosianFd, katzFd, higuchiFd, and detrendedFluc. A brief of the features is given below:

Lempel-Ziv Complexity (lempelZivComp)

Lempel-Ziv Complexity quantifies the complexity of a finite sequence based on how difficult it is to compress. A higher LZC value indicates more randomness in the signal.

Equation:

$$lempelZivComp = \frac{C(n)}{\frac{n}{log_2(n)}}$$

Where:

- C(n): Number of distinct substrings in the sequence
- n: Length of the sequence

e-ISSN: 2583-0023

Hjorth Mobility (hjorthMob)

Hjorth Mobility is a time-domain descriptor that measures the mean frequency or signal variability.

Equation:

$$hjorthMob = sqrt(\frac{Var(dx)}{Var(x)})$$

Where:

- Var(dx): Variance of the first derivative of the signal
- Var(x): Variance of the signal

Hjorth Complexity (hjorthComp)

Hjorth Complexity measures the deviation of a signal from a pure sine wave. It reflects the signal's waveform shape complexity.

Equation:

$$hjorthComp = \frac{Mobility(dx)}{Mobility(x)}$$

Where:

- Mobility(dx): Hjorth mobility of the signal's derivative
- Mobility(x): Hjorth mobility of the original signal

Fisher Information (fisherInfo)

Fisher Information quantifies the order or structure in a signal. It is sensitive to small-scale variations and is inversely related to entropy.

Equation:

$$fisherInfo = \sum \frac{(P_{i+1} - P_i)^2}{P_i}$$

Where:

- P_i: Probability of the i-th state in the signal's probability distribution

Petrosian Fractal Dimension (petrosianFd)

Petrosian Fractal Dimension provides a fast estimation of signal complexity based on the number of sign changes in the signal's derivative.

Equation:

$$petrosianFd = \frac{log_{10}(n)}{log_{10}(n) + log_{10}(\frac{n}{n + 0.4 * N\Delta})}$$

Where:

- n: Length of the signal
- NΔ: Number of sign changes in the signal derivative

Katz Fractal Dimension (katzFd)

Katz's method calculates the fractal dimension of a signal using the geometric relationship between the signal's length and the distance between its points.

Equation:

$$katzFd = \frac{log_{10}(\frac{L}{a})}{log_{10}(\frac{d}{a})}$$

Where:

- L: Total length of the curve
- a: Average distance between successive points
- d: Diameter (maximum distance between the first point and any other point)

Higuchi Fractal Dimension (higuchiFd)

Higuchi's method estimates the fractal dimension by analysing the length of the time series across different scales.

Equation:

$$higuchiFd = slope\ of\ log(L(k))\ vs.\ log(\frac{1}{k})$$

Where:

- L(k): Average length of the signal at scale k

Detrended Fluctuation (detrendedFluc)

Detrended Fluctuation Analysis measures the presence of long-range correlations in a signal by detrending local segments and computing the root-mean-square fluctuation.

Equation:

$$detrendedFluc = sqrt(\frac{1}{N \times \sum(x(t) - x\_fit(t))^2})$$

Where:

- s: Segment size
- x(t): Original signal
- x_fit(t): Local trend in each segment
- N: Total number of points

Table 2. Experiment and Selected Features

Experiment	Selected Feature Group(s) for the experiments
STP	STP features from hypnogram only
TD	All TD features from both EEG channels C3 and C4
STP_TD	Collection of all STP and TD features
TDC3	TD features from C3 channel
TDC4	TD features from C4 channel
P_Value	Features selected by P_Value<0.05
AUC	Features selected by AUC><0.5
MI	Features selected by MI><0.0
(AUC/MI)_Sel	AUC or MI features selected based on the number of features equal to the number of features selected by P_Value

Sleep Stage Transition Probability (STP)

On the other hand, for the hypnogram, the STP were calculated. A hypnogram is already a compressed form of a physiological signal. The STP features are more compressed and calculated from the ratio of the number of transition counts. The following shows the details of STP calculation [28]:

$$i \rightarrow j = \frac{C(i \rightarrow j)}{\sum_{k=W}^{REM} C(i \rightarrow k)}$$

Where i and j indicate any of the sleep stages [W, N1, N2, N3, REM] and C(i→j) means the transition count (number of transitions) from sleep stage i to stage j.

Journal of Pharmaceutical Research and Innovation (JPRI)
Volume 6, Issue 1, January 2026
e-ISSN: 2583-0023

For simplicity, the stage transition probabilities are kept simple and limited to 2-stage transitions. Two versions of these features are fed to the ML models- one is the features without feature selection, and the other is after selecting the significant features.

Feature Selection

The features extracted from the previous step are transferred directly into the ML models, and at the same time, feature selection was done before the data were fed into the ML models. For feature selection, we used three approaches: P-value, Area Under the ROC (receiver operating curve) Curve (AUC) and Mutual Information (MI). Based on the P-value (<0.05), a total of 25 features from the feature group were selected, and for the other two approaches (AUC>0.5 and MI>0), there are more features selected (AUC=38 and MI=41) for an experiment. Due to an unequal number of features and for better comparison, the same number of top features (25) from each approach were also selected for TD and STP features for other experiments. From the individual EEG channel's perspective, 6 TD features from each channel were selected for the respective experiments. For some experiments, a specific number of features were selected from a particular category of features, such as TD and STP. For another set of experiments, we selected features from all the selected channels and some individual channels to compare the results for each feature selection criterion. A list of experiments and selected features is presented in Table 2.

Table 3. Models and Parameters for GridSearch

Model	Hyperparameters and parameter values
SVM_Linear	{'kernel': ['linear'], 'C': [0.1, 1, 10]}
SVM_RBF	{'kernel': ['rbf'], 'C': [0.1, 1, 10], 'gamma': ['scale', 0.01, 0.001]}
SVM_Poly	{'kernel': ['poly'], 'C': [0.1, 1], 'degree': [2, 3]}
NB	{}
KNN	{'n_neighbors': [3, 5, 7], 'weights': ['uniform', 'distance']}
DT	{'max_depth': [None, 3, 5, 10, 15], 'criterion': ['gini', 'entropy']}
RF	{'n_estimators': [10, 20, 50], 'max_depth': [None, 3, 5, 10, 15]}
XGB	{'n_estimators': [10, 20, 50], 'max_depth': [3, 5, 10, 15], 'learning_rate': [0.05, 0.1]}

ML Classification

For all the different groups of selected features, several experiments were run using a set of ML models. The ML models used in this study are Support Vector Machine (SVM) classifiers with three different kernels-linear (SVM_Linear), poly (SVM_Poly) and RBF (SVM_RBF). Naieve Bayes (NB), K-Nearest Neighbours (KNN), Decision Tree (DT), Random Forest (RF) and eXtreme Gradient Boosting (XGB). A grid search cross-validation (CV) was applied for suitable parameter optimization as an internal CV. Externally, we used a 10-fold stratified CV that completes a nested (CV) technique for model training and validation. A list of parameters and their values to be optimized is presented in Table 3.

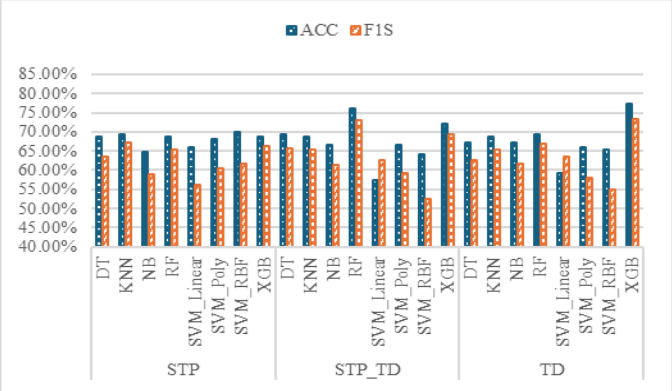

Figure 5. Performance scores for the ML models for the feature sets STP, STP_TD and TD (both EEG channels) without feature selection. Scores are presented as ACC and F1S in percentage

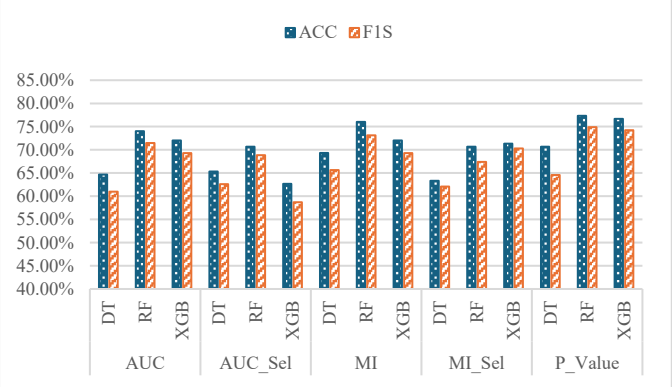

Figure 6. Performance scores for the ML models for the feature set STP_TD (both EEG channels) with feature selection using AUC, MI and P-Value. Scores are presented as ACC and F1S in percentage

Performance Metrics

The performances of the classifiers were measured using various performance measurement metrics; however, only the accuracies (ACC) and F1 scores (F1S) were presented in this article. Since the ACC and F1S scores give an overall correctness of the classifier without and with considering the misclassifications. The performance metrics were calculated using the following equations:

$$ACC = \frac{TP + TN}{TP + FN + TN + FP}$$

Where, TP (true positive)=total positive (insomnia) samples correctly identified as positive by an ML model, FN (false negative)=total positive samples misclassified as negative (healthy), TN (true negative)=total negative samples

JPRi
JOURNAL OF PHARMACEUTICAL RESEARCH AND INNOVATION
e-ISSN: 2583-0023
Journal of Pharmaceutical Research and Innovation (JPRI)
Volume 6, Issue 1, January 2026

correctly identified as negative, and FP (false positive)=total negatives misclassified as positive.

$$F1S = 2 \times \frac{PREC \times REC}{PREC + REC}$$

Where, $PREC = \frac{TP}{TP+FP}$ and $REC = \frac{TP}{TP+FN}$.

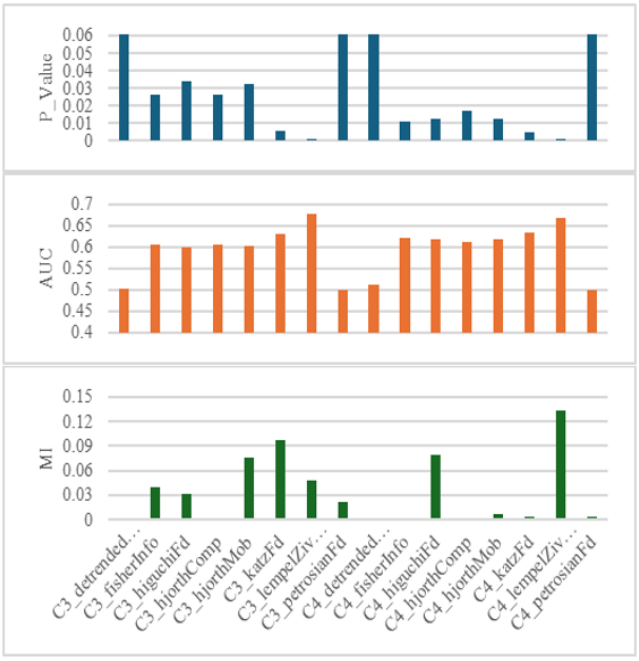

a) Feature/statistical importance scores P-Value, AUC and MI for the corresponding TD features 2 EEG channels

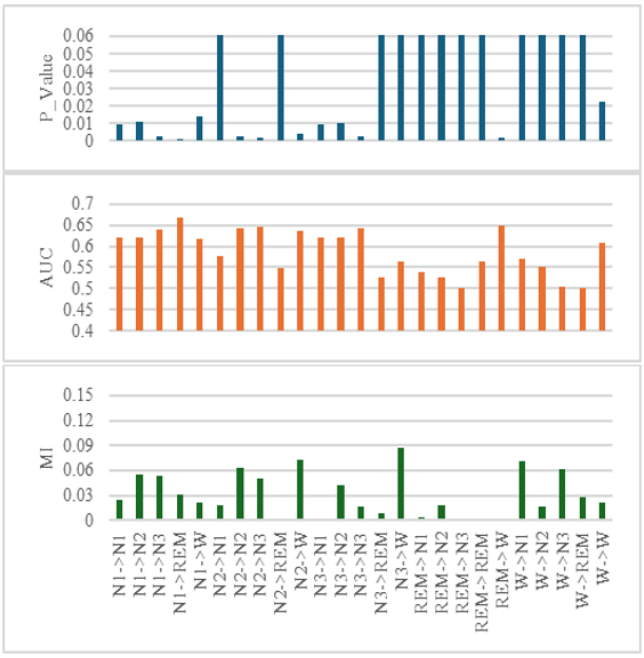

b) Feature/statistical importance scores P-Value, AUC and MI for the corresponding STP features from the hypnogram

Figure 7. Feature/statistical importance scores, P-value, AUC and MI for the corresponding features. Subplot a) presents the feature significance scores for the EEG, and b) presents the same for the hypnogram

RESULTS AND DISCUSSIONS

This section describes the results and comparison of different results achieved from the experiments. The results contain the experiments conducted with all the features and the features selected using various feature selection methods described earlier. All the plots in Figure. 5 to Figure. 9 represent the performance scores (in ACC and F1S) for corresponding ML models based on different feature groups along the X-axis (except for Figure. 6, where the X-axis represents the feature selection methods). The green bars in the plots represent the ACC scores, and the magenta bars denote the F1S for the corresponding models.

Figure. 5 shows the performance scores of eight different ML models (mentioned earlier) for three feature groups, namely, STP features, TD nonlinear features collected from two central EEG channels (C3 and C4), and STP_TD, a combination of STP and TD features. It shows that the ML models, on average, perform comparatively better for TD features. Even though the STP features do not perform better on their own, combining with the TD features, STP_TD features perform better than any other standalone feature groups. SVM and DT models are found to be underperforming in TD features; on the other hand, the KNN and NB models are better performing with the STP feature. From a generalized perspective, the ensemble models, such as RF and XGB, perform better than the traditional ML models in almost all the feature groups. The XGB model is found to be better with TD features, and the RF model is better with STP_TD features. Hence, we will continue showing the results only for three ML models, and they are DT, RF and XGB.

Since we have a different number of features extracted from the EEG signal and hypnogram. Hence, it would be better to compare these performances with an equal number of features from both modalities. Therefore, Figure. 6 presents the experimental results for the selected ML models for specific feature selection approaches such as AUC, MI and P-Value. Along with that, an equal number of selected features were selected from AUC (AUC_Sel) and MI (MI_Sel). The results show that the features selected using P-values are prominent enough to produce ~75% of the ACC and F1S for multiple models. And further reducing the features from AUC and MI, to match the number of features of P-value, they reduce the overall performance of the ML models as well. Hence, as a better choice of feature selection method, P-value-based methods can be used and are chosen for the rest of the experiments.

Figure. 7 presents the statistical feature significance calculated using P-Value, AUC and MI for both TD features from the EEG and the STP features from the hypnogram. Significant features have lower P-values (<0.05) and higher AUC values (>0.5) along with higher MI. From the P-value and MI scores, it can be seen that there are more features

Journal of Pharmaceutical Research and Innovation (JPRI)
Volume 6, Issue 1, January 2026
e-ISSN: 2583-0023

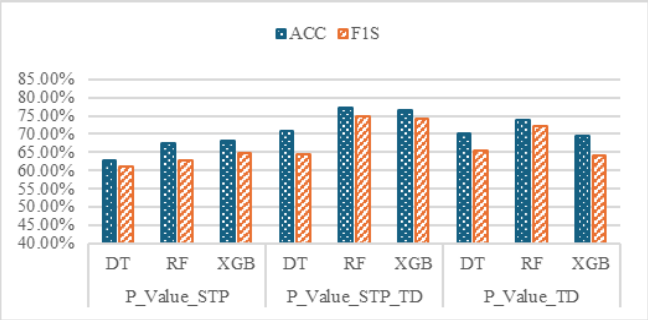

a) Performance scores for the ML models for the feature set STP, TD (both EEG channels) and STP_TD with feature selection using P-Value. Scores are presented as ACC and F1S in percentage

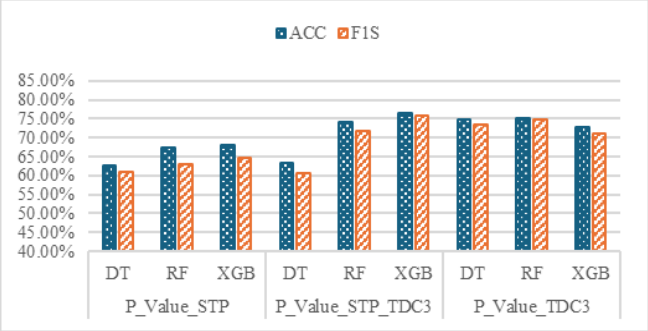

b) Performance scores for the ML models for the feature set STP, TD (for EEG channel C4) and STP_TD with feature selection using P-Value. Scores are presented as ACC and F1S in percentage

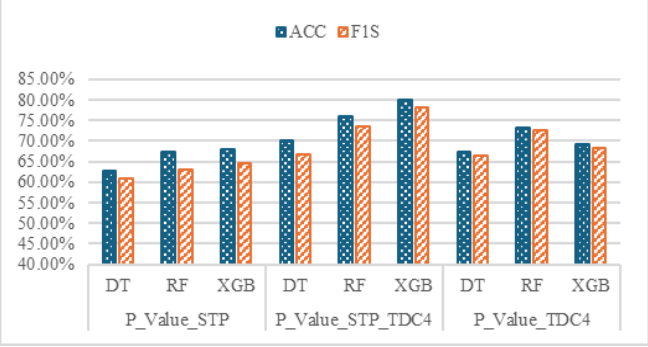

c) Performance scores for the ML models for the feature set STP, TD (for EEG channel C3) and STP_TD with feature selection using P-Value. Scores are presented as ACC and F1S in percentage

Figure 8. Performance scores for the ML models for the feature sets from the EEG signal (including two channels separately) and hypnogram, with feature selection using P-value. Scores are presented as ACC and F1S in percentage. Corresponding subplots show the performance scores for hypnogram and TD features from a) all EEG channels, b) EEG channel C4, and c) EEG channel C3

from the EEG that are significant compared to the STP features from the hypnogram. The lower AUC and MI score also indicate that the individual features are not very significant in detecting insomnia. However, combining features may help, and this benefit has been observed in the results presented in Figure. 6 already.

The subplots are presented in the Figure. 8, show the comparison of P-value-based features selected from STP, TD and STP_TD or STPTD*. And each of these subplots shows the combined TD features and selected TD features for two central EEG channels (C3 and C4). The trend of the performance scores for all channels versus the individual channels is very similar to the outcome obtained from the previous results. They clearly show that the features combined from EEG and hypnogram are comparatively better in detecting insomnia than individual feature groups from each modality. However, the scores achieved from the EEG signals of the C3 channel are found to be close to the combined features. Moreover, for the individual channels, the C4 channel achieved more benefit from the combination of EEG and hypnogram signals, reaching the ACC close to 80%. Other than that, all the experimental setups were able to gain performance scores of ~75% for both of the metrics.

As described earlier, insomnia is the most difficult sleep disorder to detect. The experimental results indicate that, due to the complexity and nature of the disorder, only the central channels may not be enough to detect insomnia, even though previous studies have found a significant relationship with central channels. Several factors might have influenced the performance scores that are not the scope of this study, such as consideration of other EEG channels, consideration of features from different feature domains (time-, frequency- and wavelet-domains), consideration of multi-stage transition dynamics of the hypnogram, etc.

CONCLUSION

Sleep architecture analysis constitutes a pivotal domain for the formulation of targeted therapeutic protocols. Among the various sleep pathologies, insomnia remains particularly diagnostically challenging. Despite the existence of multiple detection methodologies utilizing diverse physiological signals, the hypnogram has remained largely underutilized within data-driven ML frameworks, especially in multimodal configurations.

This study explores the efficacy of STP features in identifying insomnia, integrated with nonlinear TD features derived from EEG. Ensemble ML models demonstrated superior predictive performance in detecting insomnia across both single-channel and multi-channel EEG analyses.

The multimodal analysis consistently outperformed individual STP and TD feature sets, with results indicating a measurable improvement in ACC scores, ranging from 2% to 12%, for the XGBoost model. Collectively, these findings suggest that while two-stage STP features may lack the diagnostic sensitivity of powerful standalone use, they serve as a powerful adjunct when synthesized with TD features for enhanced insomnia detection.

Acknowledgements

The funding for this conference publication is sponsored by Deakin University, Australia. We would like to thank Coventry University, UK and Deakin University, Australia, for the support of one of the authors for this project. We would also like to acknowledge the owners and providers of the SDRC data that we are using in this study (Available on: https://data.mendeley.com/datasets/3hx58k232n/4).

REFERENCES

[1] Loomis, A. L., Harvey, E. N., and Hobart, G. A., 1937, Cerebral states during sleep, as studied by human brain potentials. Journal of Experimental Psychology, 21(2), 273–287.

[2] Yoneyama, M., Okuma, Y., Utsumi, H., Terashi, H., and Mitoma, H., 2014, Human turnover dynamics during sleep: statistical behavior and its modeling. Physical Review E, 89(3), 032721.

[3] Olbrich, E., Achermann, P., and Wennekers, T., 2011, The sleeping brain as a complex system. Philosophical Transactions of the Royal Society A, Oct 13, 1–12.

[4] Krueger, J. M., Obál, F., Kapás, L., and Fang, J., 1995, Brain organization and sleep function. Behavioural Brain Research, 69(1–2), 177–185.

[5] Colten, H. R., Altevogt, B. M., and Institute of Medicine (US) Committee on Sleep Medicine and Research, 2006, Functional and Economic Impact of Sleep Loss and Sleep-Related Disorders. National Academies Press, Washington DC. Available at: https://www.ncbi.nlm.nih.gov/books/NBK19958/ (Accessed 26 Nov 2024).

[6] Skaer, T. L., and Sclar, D. A., 2012, Economic implications of sleep disorders. PharmacoEconomics, 28(11), 1015–1023.

[7] Léger, D., 2000, Public health and insomnia: economic impact. Sleep, 23(1), 1–7.

[8] Hillman, D., Mitchell, S., Streatfeild, J., Burns, C., Bruck, D., and Pezzullo, L., 2018, The economic cost of inadequate sleep. Sleep, 41(8), 1–13.

[9] Liu, Y., Wheaton, A. G., Chapman, D. P., Cunningham, T. J., Lu, H., and Croft, J. B., 2016, Prevalence of healthy sleep duration among adults — United States, 2014. MMWR Morbidity and Mortality Weekly Report, 65(6), 137–141.

[10] Luca, G. et al., 2015, Age and gender variations of sleep in subjects without sleep disorders. Annals of Medicine, 47(6), 482–491.

[11] Luo, X., Zhou, B., Shi, J., Li, G., and Zhu, Y., 2024, Effects of gender and age on sleep EEG functional connectivity differences in subjects with mild difficulty falling asleep. Frontiers in Psychiatry, 15, 1433316.

[12] V, D., and G, J. M., 2024, Integrative computational intelligence techniques for insomnia and sleep stage recognition from ECG data. Indian Scientific Journal of Research in Engineering and Management, 8(11), 1–7.

[13] Sharma, N., Sharma, M., Telangore, H., and Acharya, U. R., 2024, Automated accurate insomnia detection system using wavelet scattering method with ECG signals. Applied Intelligence, 54(4), 3464–3481.

[14] Bin Heyat, M. B., et al., 2020, Progress in detection of insomnia sleep disorder: a comprehensive review. Current Drug Targets, 22(6), 672–684.

[15] Qu, W., et al., 2021, Single-channel EEG based insomnia detection with domain adaptation. Computers in Biology and Medicine, 139, 104989.

[16] Chatur, A., Haghi, M., Ganapathy, N., Taherinejad, N., Seepold, R., and Madrid, N. M., 2024, Advanced classifiers and feature reduction for accurate insomnia detection using multimodal dataset. IEEE Access, 12, 1–9.

[17] Hanif, U., Gimenez, U., Cairns, A., Lewin, D., Ashraf, N., and Mignot, E., 2023, Automatic detection of chronic insomnia from polysomnographic and clinical variables using machine learning. Proceedings of the IEEE Engineering in Medicine and Biology Society (EMBS), pp. 1–5.

[18] Tripathi, P., et al., 2022, Ensemble computational intelligence for insomnia sleep stage detection via the sleep ECG signal. IEEE Access, 10, 108710–108721.

[19] Sharma, M., Anand, D., Verma, S., and Acharya, U. R., 2023, Automated insomnia detection using wavelet scattering network technique with single-channel EEG signals. Engineering Applications of Artificial Intelligence, 126, 106903.

[20] Swihart, B. J., Caffo, B., Bandeen-Roche, K., and Punjabi, N. M., 2008, Characterizing sleep structure using the hypnogram. Journal of Clinical Sleep Medicine, 4(4), 349–355.

[21] King, C., 1980, Sleep hypnogram and sleep analysis: a rapid, inexpensive procedure. Sleep, 3(1), 93–94. Available at: https://academic.oup.com/sleep/article/3/1/93/2750188 (Accessed 3 Jan 2024).

[22] Memar, P., and Faradji, F., 2018, A novel multi-class EEG-based sleep stage classification system. IEEE Transactions on Neural Systems and Rehabilitation Engineering, 26(1), 84–95.

[23] Kim, S. W., Lee, K., Yeom, J., Lee, T. H., Kim, D. H., and Kim, J. J., 2020, Wearable multi-biosignal analysis integrated interface with direct sleep-stage classification. IEEE Access, 8, 46131–46140.

[24] Habib, A., Motin, M. A., Penzel, T., Palaniswami, M., Yearwood, J., and Karmakar, C., 2022, Performance of a convolutional neural network derived from PPG signal in classifying sleep stages. IEEE Transactions on Biomedical Engineering, XX(X), 1–15.

[25] Chaparro-Vargas, R., Ahmed, B., Wessel, N., Penzel, T., and Cvetkovic, D., 2016, Insomnia characterization: from hypnogram to graph spectral theory. IEEE Transactions on Biomedical Engineering, 63(10), 2211–2219.

[26] Bianchi, M. T., Cash, S. S., Mietus, J., Peng, C. K., and Thomas, R., 2010, Obstructive sleep apnea alters sleep stage transition dynamics. PLoS One, 5(6), e11356.

[27] Wei, Y., et al., 2017, Sleep stage transition dynamics reveal specific stage 2 vulnerability in insomnia. Sleep, 40(9), 1–7.

[28] Schlemmer, A., Parlitz, U., Luther, S., Wessel, N., and Penzel, T., 2015, Changes of sleep-stage transitions due to ageing and sleep disorder. Philosophical Transactions of the Royal Society A: Mathematical, Physical and Engineering Sciences, 373(2034).

[29] Kishi, A., et al., 2020, Sleep stage dynamics in young patients with sleep bruxism. Sleep, 43(1), 1–12.

[30] Feinberg, I., 1974, Changes in sleep cycle patterns with age. Journal of Psychiatric Research, 10(3–4), 283–306.

[31] Ali, E., Angelova, M., and Karmakar, C., 2024, Epileptic seizure detection using CHB-MIT dataset: the overlooked perspectives. Royal Society Open Science, 11(6), 230601.